



# A novel mouse model of orthotopic extrahepatic cholangiocarcinoma confirmed with molecular imaging

Xiaodong Song<sup>1,2</sup>, Zili Shao<sup>1</sup>, Menglin Han<sup>1</sup>, Huihong Liang<sup>1</sup>

<sup>1</sup>Department of Hepatobiliary Surgery, The Second Affiliated Hospital of Guangzhou Medical University, Guangzhou 510260, China; <sup>2</sup>Key Laboratory of Molecular Imaging, Institute of Automation, Chinese Academy of Sciences, Beijing 100190, China

**Contributions:** (I) Conception and design: All authors; (II) Administrative support: None; (III) Provision of study materials or patients: None; (IV) Collection and assembly of data: None; (V) Data analysis and interpretation: None; (VI) Manuscript writing: All authors; (VII) Final approval of manuscript: All authors.

**Correspondence to:** Prof. Huihong Liang, Professor of the Department of Hepatobiliary Surgery, The Second Affiliated Hospital of Guangzhou Medical University, No. 250, Changgang Road, Guangzhou 510260, China. Email: beanth@163.com.

**Background:** Cholangiocarcinoma (CCA) is the second most common primary hepatic malignancy in humans. Although early-stage CCA can be managed with surgery, CCA is considered incurable at advanced stages and results in poor quality of life and overall survival. A good orthotopic CCA animal model is essential to perform basic studies investigating CCA in order to understand the molecular pathways that underlie cancer development, and to develop new therapies for the prevention and treatment of CCA. However, to the best of our knowledge, orthotopic extrahepatic CCA animal models have not yet been reported in the literature.

**Methods:** In this study, we established an orthotopic extrahepatic CCA model in mice using a two-step surgical procedure.

**Results:** The characteristics of this model were confirmed using molecular imaging and histological analysis.

**Conclusions:** We believe that this CCA animal model, which can be established quickly, easily, and with good reproducibility, will help guide research on novel diagnostic and treatment strategies for extrahepatic CCA.

**Keywords:** Extrahepatic cholangiocarcinoma (extrahepatic CCA); xenograft; orthotopic; mice model; molecular imaging

Submitted Nov 07, 2018. Accepted for publication Mar 12, 2019.

doi: 10.21037/tcr.2019.03.19

**View this article at:** <http://dx.doi.org/10.21037/tcr.2019.03.19>

## Introduction

Cholangiocarcinoma (CCA) is the second most common primary hepatic malignancy (1). Anatomically, CCA can be classified into intrahepatic CCA and extrahepatic CCA on the basis of the tumor location within the biliary tree (2). Approximately 80–90% (3) of CCAs develop in extrahepatic locations, and extrahepatic CCA differs from intrahepatic CCA in terms of clinical presentation, etiopathogenesis, molecular signatures, and therapeutic method (4). Because of the unique anatomical position of the extrahepatic bile duct, extrahepatic CCA displays specific clinical features (5). Tumor enlargement may obstruct the common bile duct and

results in obstructive jaundice, which leads to cholestatic hepatic damage (5) (*Figure 1*). Furthermore, the malignant tumor can easily invade the surrounding organs like the pancreas and duodenum, and metastasize to lymphatic tissue and the portal vein, leading to a complex disease state and very poor prognosis. The incidence and mortality rates of CCA are currently increasing worldwide (6). Effective therapies for CC treatment are surgical extirpation (7,8) and liver transplantation (9). However, most CCA patients are diagnosed at an advanced stage, resulting in a missed surgical opportunity. Advanced CCA has an extremely poor prognosis, with a median survival after the onset of symptoms of less than 24 months (10). As a

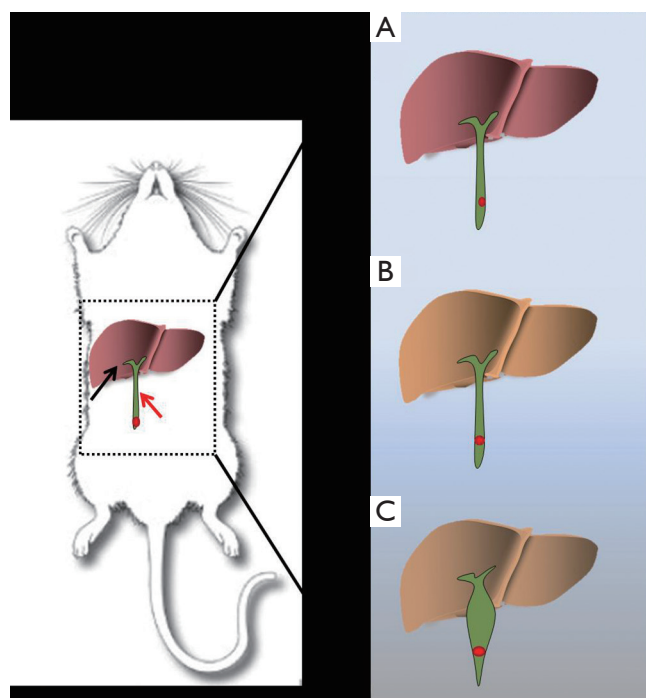


**Figure 1** The development of orthotopic extrahepatic cholangiocarcinoma.

result, early diagnosis and effective therapy are essential for optimal management of CCA. Recently, studies utilizing novel theranostic technologies such as those involving molecular biology (11,12), stem cell technology (13,14), nanotechnology (15,16), genetic modulation technology (17,18), small interfering RNA technology (19,20), tumor targeted (21,22) and cytotoxic therapy (23,24) have yielded new insights and approaches to this lethal disease. However, a reliable animal model of extrahepatic CCA has still not been established. Therefore, there is an urgent need for the establishment of an orthotopic CCA animal model.

Mice are the optimal choice for the establishment of animal models of disease because of their small size, breeding capacity, physiologic and molecular similarities to humans, and susceptibility to gene targeting (25). At present, three kinds of mouse models are used in basic cancer research: carcinogen-induced, genetically modified, and xenograft models. Establishment of carcinogen-induced models is time-consuming with a low success rate. Genetically modified models are expensive to establish. Moreover, they do not exhibit progressive precursor lesions in the biliary tract and do not consistently exhibit the common genetic lesions observed in human CCA (26).

Traditional xenograft models comprise subcutaneous xenografts and orthotopic xenografts. In CCA studies, the subcutaneous model is more widely used (27) because of the convenience of the surgery and subcutaneous injection of CCA cell lines into the flank or femoral area of immunodeficient mice, which are usually athymic nude or severe combined immunodeficient (SCID) mice (28). In addition, endpoints for determining the establishment of this model are easier to measure than they are in orthotopic models. The extensive use of fluorescent protein techniques has made it easier to measure these endpoints. Although subcutaneous models may be useful for some types of studies that investigate cancer cell behavior during tumor progression, they have some key drawbacks. For example, they do not reproduce critical tumor—stroma interactions in CCA and cannot be used to investigate spontaneous distant metastasis. In comparison, the most remarkable advantage of the orthotopic model is that it accurately mimics CCA tumorigenesis and development. Orthotopic intrahepatic CCA patient-derived xenograft (PDX) model have been studied (29), it could well reflect the histology and genetic characteristics of the primary tumor.

Current orthotopic xenograft models have several drawbacks. For example, the current orthotopic CCA model cannot distinguish between intrahepatic CCA and extrahepatic CCA (30); all CCA *in vivo* studies use an intrahepatic orthotopic CCA model while excluding extrahepatic CCA, which constitutes the majority of human CCA cases. In addition, the reported inoculating method is not reliable. The current traditional method is similar to that used in xenograft orthotopic hepatocarcinoma models (11); a cancer cell suspension is injected into the hepatic subcapsular space rather than being specifically targeted to the bile duct. This results in the inoculated cancer cells growing outside the bile duct because the intrahepatic bile duct is too small for injection without guidance. CCA is a malignant neoplasm derived from biliary epithelial cells of the inner bile duct, and a suitable animal model should mimic actual tumorigenesis and the surrounding microenvironment to enable researchers to investigate the organotypical interactions between CCA cells and surrounding stroma. Some studies (31) have transplanted BDE cells, which is an immortalized rat cholangiocyte cell line, via the bile duct into the liver of rats and used this model to determine the therapeutic efficacy of potential treatments for intrahepatic CCA. This illustrates the importance of inoculation with cancer cells via the bile duct in the investigation of CCA.

In order to resolve the aforementioned problems, we established a novel orthotopic extrahepatic CCA mouse model. In contrast to the carcinogen-induced model, the establishment of our orthotopic model is quick, requiring only about 7 days. Thus, the experimental method for the establishment of this novel animal model is simple and reproducible, enabling its adaptability in a wide array of studies. To our knowledge, this is first report describing the establishment of an orthotopic extrahepatic CCA mouse model. Tumor formation occurred specifically in the common bile duct, which reflects extrahepatic CCA. This model provides a practical basis for studying various biological aspects of extrahepatic CCA, including cancer cell proliferation, metastasis, tumor microenvironment, and efficacy of novel therapeutic approaches.

## Methods

### *Cell culture and pre-inoculation procedures*

The QBC939 cell line, a human CCA cancer cell line marker with luciferase, was purchased from the Genechem Shanghai Co., Ltd. Regular QBC939 cells were cultured in Dulbecco's modified Eagle medium (Gibco®, Australia), supplemented with 10% fetal bovine serum (Gibco®, Australia), 1% penicillin-streptomycin (Gibco®, Australia). All cells were cultured in an atmosphere of 5% CO<sub>2</sub> at 37 °C. Cell lines were used for inoculation after being washed with PBS and digested with trypsin-EDTA (Gibco®, Australia). The cytolymph was isolated by centrifuging at 800 rpm for 5 minutes. The supernatant was discarded, and cells were resuspended in PBS or Matrigel (Basement Membrane Matrix, Growth Factor Reduced, Phenol Red-free, BD Biosciences, USA) before inoculation. Cancer cells and Matrigel mix were stored at 4 °C to prevent congealing of Matrigel. All experiments were performed using cells in the logarithmic phase of growth.

### *Preparation of mice*

BALB/c male mice (aged 4–6 weeks, weighing 30–40 g; n=20) were acquired from Beijing Vital River Laboratory Animal Technology Co. Ltd. All experimental protocols were approved by the Institutional Animal Care and Ethics Committee of Zhujiang Hospital of Southern Medical University, and all procedures were performed in accordance with the approved guidelines. Mice were divided into 3 groups: group A (n=5), group B (n=5), and group

C (n=10). All mice received food and water ad libitum, and were housed at a temperature range of 18–29 °C and humidity range of 40–70%.

### *Establishment of extrahepatic CCA models*

The extrahepatic CCA models were established using three different protocols in order to detect the optimal method for model establishment. In group A, cancer cells suspended in PBS were inoculated slowly into the common bile duct. In group B, the distal common bile duct was ligatured 3 days before the inoculation of cancer cells. In group C, cancer cells were inoculated with Matrigel, and ligation of the common bile duct was performed 3 days before inoculation, as in group B. The surgery details are described below.

Mice in groups B and C first underwent ligation of the common bile duct to induce choledochectasia. Mice were anesthetized by intraperitoneally injecting 2 µL/g of 10% chloral hydrate. Then, the skin was incised and the abdominal wall and peritoneum were kept away from the abdominal wall muscle and vessels by an upper abdomen midline laparotomy performed under sterile conditions. The intestine was pushed aside, the duodenum gently was lifted out of the abdomen, and finally, the common bile duct, which lies between the duodenum and the porta hepatic, was exposed. We gently separated the common bile duct and ligatured the lower segment of the common bile duct with 5-0 silk thread. The organs were replaced, and the incision was sutured at the end (*Figure 2*).

CCA cells were injected into the common bile duct to establish the extrahepatic CCA models. In group A, 50 µL of QBC939 cell suspension in PBS was injected directly and slowly into the common bile duct. For the group B and C mice, we conducted a second surgery. Three days after the ligation, we incised the skin and peritoneum of mice that were anesthetized as in the first surgery. The dilated common bile duct could be exposed easily, guided by the ligated thread residue at the right upper abdomen from the first surgery. After separating the common bile duct carefully to avoid injury to the peripheral vessels and surrounding organs (*Figure 2*), we used an insulin pen to inject QBC939 cells suspended in PBS (group B) or in Matrigel mixture (group C). The volume of the total injection was adjusted to 50 µL. The mixing of the suspension was performed gently and slowly during the injection process in order to avoid leakage of the cancer cells outside the bile duct, since the high pressure in the bile duct might lead to its rupture. The

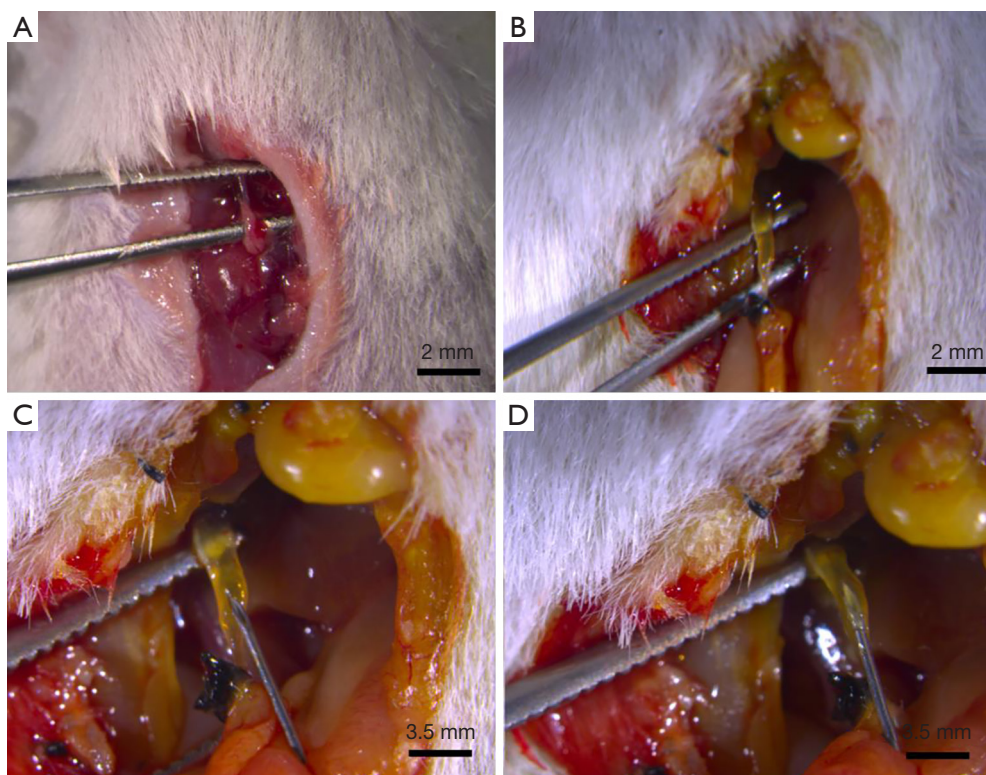


**Figure 2** Illustration of the surgical process.

**Table 1** Schedule of establishing the xenograft orthotopic extrahepatic cholangiocarcinoma model

Day 1	Day 2	Day 3	Day 4	Day 5	Day 6	Day 7
Establishment of choledochectasia model (1st surgery)	–	Inoculation of cancer cells (2nd surgery)	–	–	–	Examination of tumor growth with an IVIS spectrum imaging system and histology analysis

IVIS, in vivo imaging system.

flow of the mixed suspension into the inner the bile duct could be observed with the naked eye (Figure 2). We then put the organs back into the abdominal cavity, and sterilized and sutured the incision site as before.

#### **Verification of tumor growth in the mouse model**

Mice were observed carefully after the surgery. Four days after inoculation, tumor growth was evaluated with an IVIS spectrum imaging system (PerkinElmer, USA) after intraperitoneal injecting fluorescent protein substrate luciferin (Roche). Subsequently, histopathological examinations were performed in these tumor-bearing mice. The mice were dissected, and the dilated common bile duct

was extracted. The tissue was soaked in 4% paraformaldehyde solution for 24 h, and embedded in paraffin. Tissue sections of 4–5 mm thickness were mounted on poly-L-lysine-coated slides (Sigma-Aldrich, St. Louis, MO, USA). Sections were deparaffinized with xylene, rehydrated with decreasing concentrations of ethanol, equilibrated in water, and subsequently stained with hematoxylin and eosin.

The detailed schedule and results of group C are described in Table 1.

## **Results and discussion**

### ***The establishment of the choledochectasia model***

The average diameter of the common bile duct in BALB/

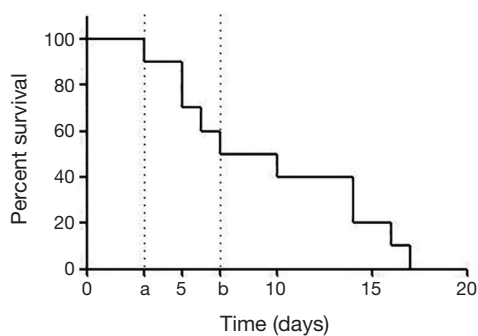


**Figure 3** The survival rate of mice at the different surgery stages.

C mice is approximately 0.1 mm. The original diameter of the common bile duct in the mice used in this study was very small, as is shown in *Figure 2A*. Considering this small diameter, we designed a two-step surgical procedure. In the first step, we established a choledochectasia mouse model.

After the first common bile duct ligation surgery, mice manifested several symptoms of obstructive jaundice: lack of appetite, hair disorder, and urine that was a darker shade of yellow. This indicated that the obstructive jaundice mouse model was established successfully. The high pressure in the bile duct due to the obstructive jaundice persisted, resulting in dilation, with an approximate increase in diameter to 0.5 mm (*Figure 2B*) within 2 days after ligaturing the common bile duct. We concluded that 2 days was an appropriate period on the basis of our findings and those of a previous report (32) indicating that the diameter of bile duct peaked on the third day after surgery and was stable thereafter.

In the second step, we inoculated QBC939 cells into the lower section of common bile duct (*Figure 2C*). We were able to easily imbed the insulin needle into the common bile duct to inject the QBC939 cell suspension easily and observe the suspension flow inner the common bile duct by naked eyes (*Figure 2D*). At the second surgery, the common bile duct dilated up to 3 mm in diameter on average.

#### **Observations in the mice after the two-step surgery**

All mice recovered quickly from anesthesia, displayed normal behavior after the first surgery, and manifested signs of obstructive jaundice as described above. However, some mice died (n=5), especially after the second surgery. The survival rate of group C mice is shown in *Figure 3*.

The post-mortem dissection results revealed several reasons for the mortality of group C mice: obstructive

jaundice (n=3), injury during operation (n=1), and attacks by other mice in same cage (n=1). Obstructive jaundice due to common bile duct ligation is known to induce biliary inflammation, fibrosis, and cholestatic liver injury (33). In the mouse that died because of injury during surgery, the fragile bile duct was torn during the process of isolation. One mouse died because it was attacked by other mice in the same cage. Each mouse had a different recovery time from surgery and anesthesia. The mice with slower recovery times were susceptible to attack by the fast-recovering mice in the same cage, even though they underwent surgery at the same time. Therefore, the mice should be placed in separate cages after surgery. All dissected mice displayed abundant ascites, and liver and gall bladder bile stasis. One of the mice experienced gangrenous cholecystitis due to the excess pressure in the bile duct system and bacterial toxicity.

With time and experience, the surgery time and mortality rate of this new method of orthotopic extrahepatic CCA inoculation should decrease. However, because common bile duct ligation results in a high postoperative mortality rate, probably due to traumatic pancreatitis (34), the total postoperative survival time is inevitably limited. The median survival time of our model mice was as short as 2 weeks (*Figure 3*). Thus, this model is not amenable to long-term studies. However, it does provide a novel model for the study of advanced diagnosis methods and tumorigenesis mechanisms.

#### **Imaging of tumor xenografts**

Ligation of the common bile duct prevented the flow of the cancer cell suspension with the bile into the duodenum, thus allowing the cancer cells to accumulate in the bile duct and grow into a tumor gradually. We hypothesized that tumor development would occur if the microenvironment was suitable and the cancer cells were stable at a fixed location. In the control groups A and B in our experiment, the cancer cells were dispersed and therefore, failed to form a tumor. Although the common bile duct was ligated in group B, the cancer cells were flushed by bile and dispersed into the intrahepatic bile tract.

BD Matrigel, which congeals at room temperature, stabilized the inoculated cancer cells, preventing them from being dispersed by bile. Therefore, Matrigel injected together with cancer cells resulted in the ideal outcome of reliable tumor growth. Matrigel mainly consists of laminin, collagen IV, heparan sulfate proteoglycans, entactin/nidogen, and various other growth factors. It has been

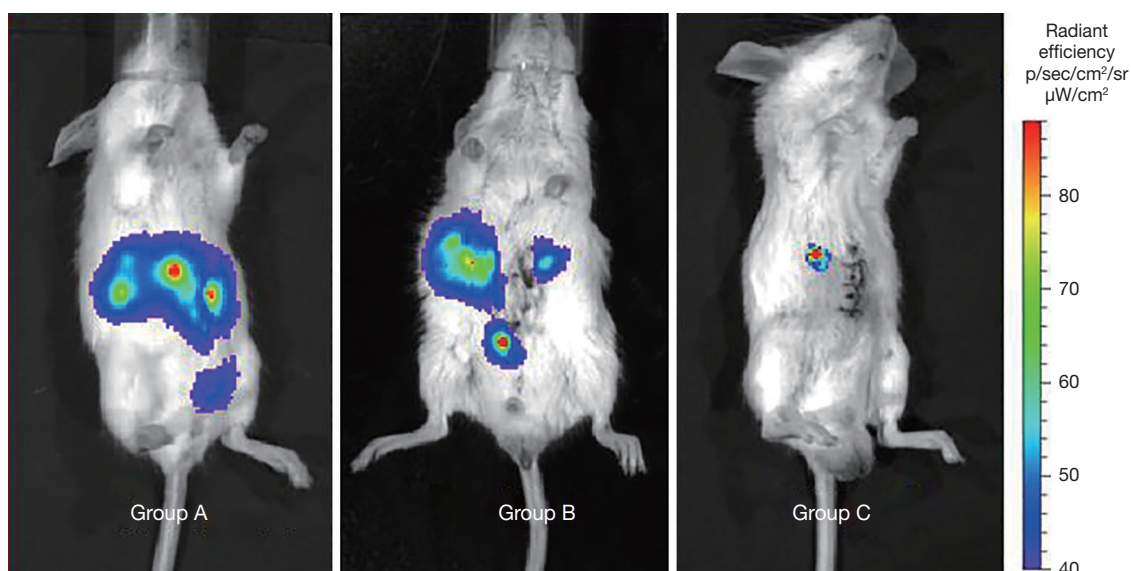


**Figure 4** IVIS spectrum imaging results. IVIS, in vivo imaging system.

demonstrated that Matrigel plays a significant role in tumor development, metastasis, and morphology, and provides a beneficial microenvironment for tumor growth (35). It is reported that co-injection with Matrigel in orthotopic xenograft models contributes to an accelerated rate of tumor growth (36). Results of IVIS spectrum imaging of group C mice, in which CCA cells were injected with Matrigel, revealed a more favorable response than that in group B and group C mice. The concentrated fluorescence signal expressed in the common bile duct was quantified individually. The average region of interest (ROI) fluorescence value in the isolated bile duct tissue after dissection was  $1.232 \times 10^4$  and  $2.049 \times 10^7$ . These fluorescence intensity values were higher than the *in vivo* values because of the decrease in fluorescence signal due to passage through the abdominal wall. The fluorescence values for the isolated dissected bile duct were consistent with the results of the hematoxylin and eosin staining, confirming tumor formation in the common bile duct.

On the fourth day after the second surgery, the mice were examined using an IVIS spectrum imaging system after an intraperitoneal injection of luciferin as a substrate. The fluorescent signal was dispersed around the abdominal cavity in groups A and B (Figure 4), which indicated that the cancer cells inoculated into the common bile duct had failed to grow into a tumor in the liver and other organs. Fluorescence in group B was more concentrated, but fluorescence signal was detected in an intrahepatic

location. Compared to the signal for groups A and B, the fluorescence signal in group C was concentrated at the precise point of the common bile duct, where the cancer cells were inoculated (Figure 4). The respective average fluorescence ROI intensity value was  $2.037 \times 10^3$  in group A,  $1.420 \times 10^3$  in group B, and  $1.232 \times 10^4$  in group C. Although all groups displayed nearly the same fluorescence ROI intensity, the fluorescent signal in the mice in group C was visible only on the right side of the body. Therefore, we considered group C as a successful candidate for an extrahepatic CCA mouse model.

#### **Confirmation of the successful establishment of the CCA mouse model**

A strong and clear fluorescence signal can be observed at the anatomical location of the common bile duct (Figure 5A) in a group C mouse, with no other interference signal. The average ROI fluorescence intensity value was  $1.232 \times 10^4$ . To confirm the exact location of fluorescence source, we dissected the mice, removed the common bile duct organ and liver individually, and then examined them separately with IVIS spectrum imaging (Figure 5B). A clear fluorescence signal was observed in the common bile duct tissue (average ROI value,  $2.049 \times 10^7$ ) demonstrating that the orthotopic extrahepatic CCA model was established successfully. The tumor grew at the tip of common bile duct as shown in Figure 5C.

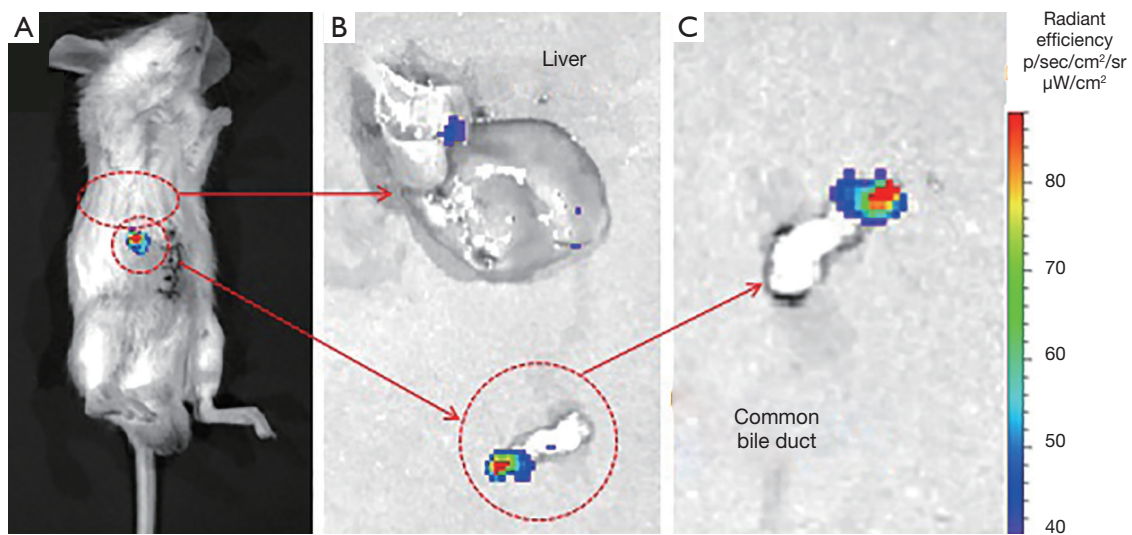


**Figure 5** IVIS spectrum imaging of the liver and common bile duct after dissection. IVIS, in vivo imaging system.

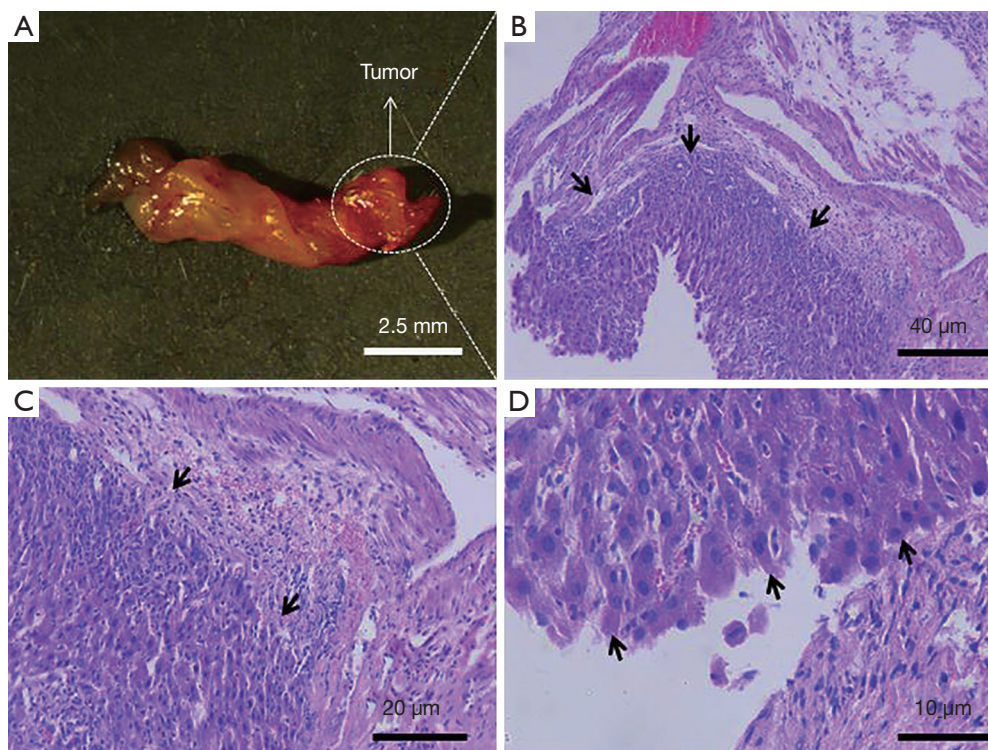


**Figure 6** Gross specimen and hematoxylin and eosin (HE)-stained pathological tissue section.

**Histopathological evaluation**

The imaging findings were confirmed by histological examination of the common bile duct tissue. In the

gross specimen (Figure 6A), the common bile duct tissue was approximately 10 mm long, and the tumor size was approximately 0.5 mm × 0.5 mm on average. Serial hematoxylin and eosin-stained sections of the bile duct

confirmed tumor formation. The cancer cells in the tumor region were disorganized, with a markedly altered nucleus-to-cytoplasm ratio, which is a specific malignancy characteristic, and could be distinguished from normal tissue by microscopic observation (*Figure 6*).

## Conclusions

Extrahepatic CCA is a complex and challenging disease both in basic research and in clinical practice. A reliable animal model is essential for conducting advanced research in order to bridge the gap between *in vitro* experiments and human applications. To address this necessity, we established an orthotopic extrahepatic CCA mice model. In our mouse model, the tumor grew specifically in the common bile duct, which accurately reflects extrahepatic CCA. The mouse model established in this study provides an invaluable practical model that can be used in studies investigating advanced diagnostic and therapeutic technologies for extrahepatic CCA.

## Acknowledgments

**Funding:** This work was supported by Guangzhou medical science and technology project (No. 20171A010304).

## Footnote

**Conflicts of Interest:** All authors have completed the ICMJE uniform disclosure form (available at <http://dx.doi.org/10.21037/tcr.2019.03.19>). The authors have no conflicts of interest to declare.

**Ethical Statement:** The authors are accountable for all aspects of the work in ensuring that questions related to the accuracy or integrity of any part of the work are appropriately investigated and resolved. The study was approved by the Institutional Animal Care and Ethics Committee of Zhujiang Hospital of Southern Medical University.

**Open Access Statement:** This is an Open Access article distributed in accordance with the Creative Commons Attribution-NonCommercial-NoDerivs 4.0 International License (CC BY-NC-ND 4.0), which permits the non-commercial replication and distribution of the article with the strict proviso that no changes or edits are made and the original work is properly cited (including links to both the formal publication through the relevant DOI and the license).

See: <https://creativecommons.org/licenses/by-nc-nd/4.0/>.

## References

- Gatto M, Alvaro D. New insights on cholangiocarcinoma. *World J Gastrointest Oncol* 2010;2:136-45.
- Carpizo DR, D'Angelica M. Management and extent of resection for intrahepatic cholangiocarcinoma. *Surg Oncol Clin N Am* 2009;18:289-305.
- Blechacz BR, Gores GJ. Cholangiocarcinoma. *Clin Liver Dis* 2008;12:131-50.
- Esnaola NF, Meyer JE, Karachristos A, et al. Evaluation and management of intrahepatic and extrahepatic cholangiocarcinoma. *Cancer* 2016;122:1349-69.
- Altaee MY, Johnson PJ, Farrant JM, et al. Etiologic and clinical characteristics of peripheral and hilar cholangiocarcinoma. *Cancer* 1991;68:2051-5.
- Welzel TM, McGlynn KA, Hsing AW, et al. Impact of classification of hilar cholangiocarcinomas (Klatskin tumors) on the incidence of intra- and extrahepatic cholangiocarcinoma in the United States. *J Natl Cancer Inst* 2006;98:873-5.
- Jarnagin WR, Fong Y, DeMatteo RP, et al. Staging, resectability, and outcome in 225 patients with hilar cholangiocarcinoma. *Ann Surg* 2001;234:507-17; discussion 517-9.
- Kosuge T, Yamamoto J, Shimada K, et al. Improved surgical results for hilar cholangiocarcinoma with procedures including major hepatic resection. *Ann Surg* 1999;230:663-71.
- Nakeeb A, Pitt HA, Sohn TA, et al. Cholangiocarcinoma. A spectrum of intrahepatic, perihilar, and distal tumors. *Ann Surg* 1996;224: 463-73; discussion 473-5.
- Farley DR, Weaver AL, Nagorney DM. "Natural history" of unresected cholangiocarcinoma: patient outcome after noncurative intervention. *Mayo Clin Proc* 1995;70:425-9.
- Ngernyuang N, Seubwai W, Daduang S, et al. Targeted delivery of 5-fluorouracil to cholangiocarcinoma cells using folic acid as a targeting agent. *Mater Sci Eng C Mater Biol Appl* 2016;60:411-5.
- Brito AF, Abrantes AM, Encarnacao JC, et al. Cholangiocarcinoma: from molecular biology to treatment. *Med Oncol* 2015;32:245.
- Cardinale V, Renzi A, Carpino G, et al. Profiles of cancer stem cell subpopulations in cholangiocarcinomas. *Am J Pathol* 2015;185:1724-39.
- Shuang ZY, Wu WC, Xu J, et al. Transforming growth factor-beta1-induced epithelial-mesenchymal transition

- generates ALDH-positive cells with stem cell properties in cholangiocarcinoma. *Cancer Lett* 2014;354:320-8.
15. Tang T, Zheng JW, Chen B, et al. Effects of targeting magnetic drug nanoparticles on human cholangiocarcinoma xenografts in nude mice. *Hepatobiliary Pancreat Dis Int* 2007;6:303-7.
  16. Wiedmann M, Caca K, Berr F, et al. Neoadjuvant photodynamic therapy as a new approach to treating hilar cholangiocarcinoma: a phase II pilot study. *Cancer* 2003;97:2783-90.
  17. Yamanaka S, Campbell NR, An F, et al. Coordinated effects of microRNA-494 induce G(2)/M arrest in human cholangiocarcinoma. *Cell Cycle* 2012;11:2729-38.
  18. Olaru AV, Ghiaur G, Yamanaka S, et al. MicroRNA down-regulated in human cholangiocarcinoma control cell cycle through multiple targets involved in the G1/S checkpoint. *Hepatology* 2011;54:2089-98.
  19. Zhang K, Chen D, Wang X, et al. RNA interference targeting slug increases cholangiocarcinoma cell sensitivity to cisplatin via upregulating PUMA. *Int J Mol Sci* 2011;12:385-400.
  20. Zheng T, Hong X, Wang J, et al. Gankyrin promotes tumor growth and metastasis through activation of IL-6/STAT3 signaling in human cholangiocarcinoma. *Hepatology* 2014;59:935-46.
  21. Inufusa H, Adachi T, Suzuki M, et al. Generation of a monoclonal antibody that inhibits the procoagulant activity of various cancer cell lines. *Cancer* 1998;82:1563-9.
  22. Nagamitsu A, Greish K, Maeda H. Elevating blood pressure as a strategy to increase tumor-targeted delivery of macromolecular drug SMANCS: cases of advanced solid tumors. *Jpn J Clin Oncol* 2009;39:756-66.
  23. Frampton GA, Lazcano EA, Li H, et al. Resveratrol enhances the sensitivity of cholangiocarcinoma to chemotherapeutic agents. *Lab Invest* 2010;90:1325-38.
  24. Müller A, Barat S, Chen X, et al. Comparative study of antitumor effects of bromelain and papain in human cholangiocarcinoma cell lines. *Int J Oncol* 2016;48:2025-34.
  25. Reiberger T, Chen Y, Ramjiawan RR, et al. An orthotopic mouse model of hepatocellular carcinoma with underlying liver cirrhosis. *Nat Protoc* 2015;10:1264-74.
  26. O'Dell MR, Huang JL, Whitney-Miller CL, et al. Kras(G12D) and p53 mutation cause primary intrahepatic cholangiocarcinoma. *Cancer Res* 2012;72:1557-67.
  27. Kokuryo T, Senga T, Yokoyama Y, et al. Nek2 as an effective target for inhibition of tumorigenic growth and peritoneal dissemination of cholangiocarcinoma. *Cancer Res* 2007;67:9637-42.
  28. Zhang J, Han C, Wu T. MicroRNA-26a promotes cholangiocarcinoma growth by activating beta-catenin. *Gastroenterology* 2012;143:246-56.e8.
  29. Cavalloni G, Peraldo-Neia C, Sassi F, et al. Establishment of a patient-derived intrahepatic cholangiocarcinoma xenograft model with KRAS mutation. *BMC Cancer* 2016;16:90.
  30. Ko KS, Peng J, Yang H. Animal models of cholangiocarcinoma. *Curr Opin Gastroenterol* 2013;29:312-8.
  31. Blechacz BR, Smoot RL, Bronk SF, et al. Sorafenib inhibits signal transducer and activator of transcription-3 signaling in cholangiocarcinoma cells by activating the phosphatase shatterproof 2. *Hepatology* 2009;50:1861-70.
  32. Zhang SH, Liao CX, Zhang CX, et al. Establishment of a mouse model of biliary obstruction and its dynamic observations. *Nan Fang Yi Ke Da Xue Xue Bao* 2008;28:1579-81.
  33. Guicciardi ME, Gores GJ. Cholestatic hepatocellular injury: what do we know and how should we proceed. *J Hepatol* 2005;42:297-300.
  34. Kaiser AM, Saluja AK, Steer ML. Repetitive short-term obstructions of the common bile-pancreatic duct induce severe acute pancreatitis in the opossum. *Dig Dis Sci* 1999;44:1653-61.
  35. Ghajar CM, Bissell MJ. Extracellular matrix control of mammary gland morphogenesis and tumorigenesis: insights from imaging. *Histochem Cell Biol* 2008;130:1105-18.
  36. Fridman R, Kibbey MC, Royce LS, et al. Enhanced tumor growth of both primary and established human and murine tumor cells in athymic mice after coinjection with Matrigel. *J Natl Cancer Inst* 1991;83:769-74.

**Cite this article as:** Song X, Shao Z, Han M, Liang H. A novel mouse model of orthotopic extrahepatic cholangiocarcinoma confirmed with molecular imaging. *Transl Cancer Res* 2019;8(2):583-591. doi: 10.21037/tcr.2019.03.19